ISSN 1063-7834, Physics of the Solid State, 2011, Vol. 53, No. 8, pp. 1672–1679. © Pleiades Publishing, Ltd., 2011.
Original Russian Text © M.S. Molokeev, S.V. Misyul', 2011, published in Fizika Tverdogo Tela, 2011, Vol. 53, No. 8, pp. 1589–1595.

PHASE TRANSITIONS

Structural Transformations and the Critical and Noncritical Parameters during the Phase Transition in the $(NH_4)_2KWO_3F_3$ Oxyfluoride

M. S. Molokeev[a, *] and S. V. Misyul'[b, **]

[a] *Kirensky Institute of Physics, Siberian Branch, Russian Academy of Sciences, Akademgorodok, Krasnoyarsk, 660036 Russia*

* *e-mail: msmolokeev@mail.ru*

[b] *Siberian Federal University, Svobodnyi pr. 79, Krasnoyarsk, 660041 Russia*

** *e-mail: misjul@akadem.ru*

Received January 13, 2011

Abstract—The structures of two phases of the $(NH_4)_2KWO_3F_3$ crystal have been determined from X-ray diffraction data obtained for a powder sample. The profile and structural parameters have been refined according to the procedure implemented in the DDM program. The results obtained have been discussed with invoking the group-theoretical analysis of the complete order parameter condensate, which takes into account the critical and noncritical atomic orderings and allows one to interpret the experimental data. It has been found that the symmetry transformation in the crystal can be schematically represented in the form $Fm\bar{3}m \xrightarrow[(\eta, 0, 0, 0, 0, 0)]{10-10(X_5^-)} Pmmn$. This transformation is accompanied by the ordering of WO_3F_3 polyhedra and the displacement of NH_4 and K ions.

DOI: 10.1134/S1063783411080208

1. INTRODUCTION

The main structural elements in compounds of the general formula $A_2BMO_xF_{6-x}$ (where A, B = K, Rb, Cs; M = Ti, Mo, W; $x = 1, 2, 3$) are noncentrosymmetric oxyfluoride anions MO_xF_{6-x}, which, under specific conditions, allow the formation of polar structures with ferroelectric properties [1]. However, the majority of fluorine–oxygen compounds crystallize in the nonpolar phase of the cubic elpasolite-like structure with a face-centered lattice (space group $Fm\bar{3}m$, $Z = 4$) [1, 2], which, most likely, indicates a fluorine–oxygen disorder in the MO_xF_{6-x} anions. With a decrease in the temperature, the majority of the oxyfluorides undergo phase transitions of the ferroelastic or ferroelectric nature due to the ordering and small atomic displacements [1, 2].

The calorimetric investigations performed in our previous work [3] on the $(NH_4)_2KWO_3F_3$ crystal revealed the occurrence of a single second-order structural transformation at a temperature $T_0 = 235.4 \pm 0.1$ K with the change of entropy $\Delta S_0 = R\ln(1.76)$. In [3, 4], it was shown using the X-ray diffraction methods that the $(NH_4)_2KWO_3F_3$ crystal exists in the G_0 cubic phase (space group $Fm\bar{3}m$, $Z = 4$) at temperatures above $T_0 = 235.4$ K and in the G_1 monoclinic phase (space group $P2_1/n$, $Z = 2$) at temperatures below T_0. According to the structures refined in [4] for the cubic and monoclinic phases of the $(NH_4)_2KWO_3F_3$ compound, the conclusion has been drawn that the phase transition, most likely, is associated with the atomic displacements rather than with the ordering of the tetrahedral NH_4 or octahedral WO_3F_3 groups.

However, the group-theoretical analysis of the structural phase transitions from the cubic phase with space group $Fm\bar{3}m$ [5] has demonstrated that the symmetry transformation $Fm\bar{3}m \longrightarrow P2_1/n$ proposed in [4] cannot proceed as a second-order phase transition, which is in disagreement with the data obtained in [3]. Therefore, it can be assumed that the symmetry and model of the structure of the distorted phase G_1 require correction and more comprehensive structural investigation of the $(NH_4)_2KWO_3F_3$ oxyfluoride. Furthermore, the change of entropy and the results obtained in all the preceding works do not provide answers to the question as to which atoms or groups of atoms, atomic displacements or orderings, are related to the phase transition under investigation.

In order to refined the mechanism of the phase transformation occurring in the $(NH_4)_2KWO_3F_3$ crystal and to eliminate the aforementioned discrepancies, we carried out more accurate temperature X-ray powder diffraction investigations of the structural charac-

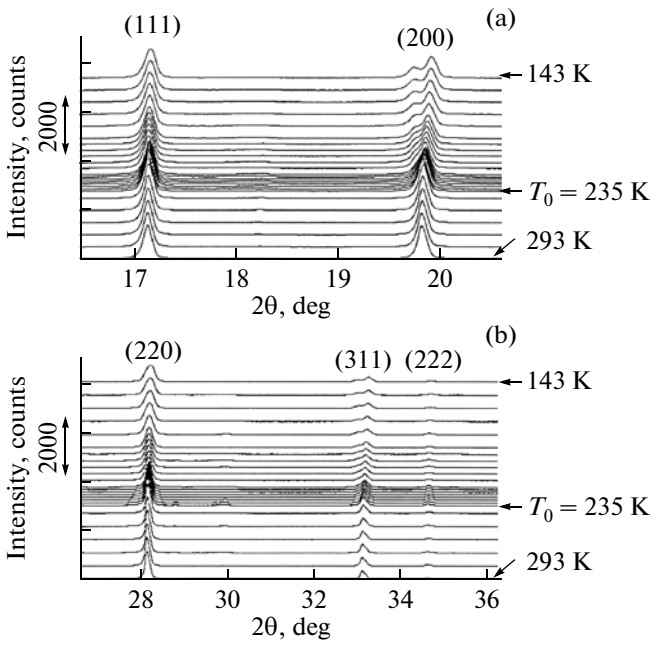

Fig. 1. Fragments of the X-ray diffraction patterns of the $(NH_4)_2KWO_3F_3$ compound with the reflections (a) (1 1 1) and (2 0 0) and (b) (2 2 0), (3 1 1), and (2 2 2) at different temperatures.

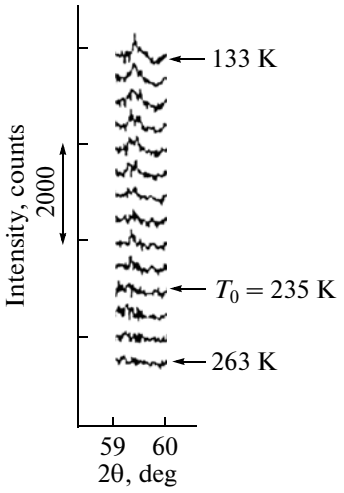

Fig. 2. A fragment of the X-ray diffraction pattern of the $(NH_4)_2KWO_3F_3$ compound in the range of the (1 4 4) reflection with variations in the temperature.

teristics of the crystal and their changes during the phase transition.

2. SAMPLE PREPARATION AND EXPERIMENTAL TECHNIQUE

The synthesis of the studied compound $(NH_4)_2KWO_3F_3$, which was described in detail in our previous papers [3, 4], was performed according to the chemical reaction $K[WO_2F_3] \cdot H_2O + 2NH_4OH \longrightarrow (NH_4)_2KWO_3F_3 + 2H_2O$.

The X-ray diffraction patterns from polycrystalline samples of the $(NH_4)_2KWO_3F_3$ compound were recorded using an Anton Paar TTK450 temperature chamber installed on a D8-ADVANCE X-ray powder diffractometer (CuK_α radiation, θ–2θ scan mode, VANTEC linear position-sensitive detector). Liquid nitrogen was used as a coolant. The scan step in the angle 2θ was equal to 0.016°, and exposure per frame was 0.3 s. The experiments were carried out at temperatures in the range from 293 to 143 K with a step varying from 2 to 10 K, depending on how close the temperature of the measurement is to the temperature of the phase transition. This made it possible reveal regularities in the variations of the structural characteristics of the crystal during the phase transition. In order to more reliably refine the structures of the parent and distorted phases at two temperatures (298 and 133 K), each being fairly different from the phase transition temperature, the exposure at each experimental step was increased to 3 s.

By applying the homology method [6] to analyzing the splitting of X-ray reflections of the parent cubic phase in the X-ray diffraction pattern with a decrease in the temperature (Figs. 1a and 1b), it can be affirmed that the symmetry of the distorted phase is either orthorhombic, or monoclinic, or triclinic.

In order to reveal superstructure reflections, we performed an additional experiment. Unfortunately, the X-ray diffraction pattern of the sample under investigation contained a large number of weak impurity reflections in the angle range up to 2θ = 50°. During cooling of the sample, small amounts of water vapors in the chamber or in the sample also gave rise to several very weak reflections from the ice. All these impurity reflections hindered the observation of superstructure reflections belonging to the $(NH_4)_2KWO_3F_3$ compound. However, in the angle range 2θ ~ 59.4°, which is free from the reflections of impurities and the ice phase, we revealed the (1 4 4) superstructure reflection (the indices are given in terms of cubic unit cell parameters). This range was thoroughly scanned. The temperature of the sample was varied in the range from 263 to 133 K. The exposure at each new temperature was increased to 10 min (Fig. 2). This made it possible to elucidate the temperature behavior of the integrated intensity of the (1 4 4) superstructure reflection (Fig. 3). For this purpose, we used the EVA program, which is implemented in the DIFFRAC-PLUS software package (Bruker).

3. EXPERIMENTAL RESULTS

A linear increase in the integrated intensity of the (1 4 4) superstructure reflection with a decrease in the

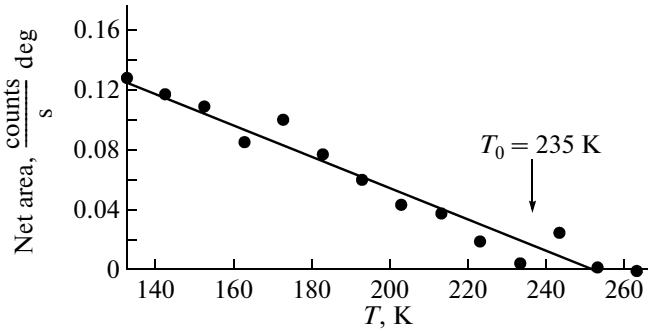

Fig. 3. Temperature dependence of the integrated intensity of the (1 4 4) superstructure reflection.

temperature beginning with $T_0 = 235$ K indicates that the dominant contribution to the intensity of this reflection is introduced by the critical order parameters. The mere fact that the (1 4 4) superstructure reflection exists points to a change in the volume of the unit cell of the crystal during the phase transition. Therefore, the splitting of X-ray reflections and the presence of superstructure reflections in the X-ray diffraction patterns suggest that the symmetry of the distorted phase of the $(NH_4)_2KWO_3F_3$ compound is either orthorhombic, or monoclinic, or triclinic with the most probable change in the volume of the primitive cell by a factor of two with respect to the volume of the unit cell of the cubic phase.

The further consideration of the experimental data will be based on the works dealing with the group-theoretical analysis of the structural phase transitions in crystals with space group $Fm\bar{3}m$ [5] and on the ISOTROPY [7] and ISODISPLACE [8] software packages. By using the data reported in [5, 7], we obtained all possible space groups of the distorted phase in the orthorhombic and monoclinic crystal systems with a twofold increase in the volume of the primitive cell (Table 1) so that the transitions to these space groups are second-order phase transitions. It should be noted that we had at once to discard triclinic space groups, because the phase transition in this case can occur only as a first-order phase transition. Thus, with allowance made for the aforementioned constraints on the symmetry of the distorted phase, we obtained six possible symmetry variants. Four out of the six variants represent monoclinic unit cells. However, none of these monoclinic unit cells gives rise to the observed

Table 1. Possible variants of the space groups and primitive cells (with a twofold increase in the primitive cell volume) of the distorted phase of the $(NH_4)_2KWO_3F_3$ compound, each corresponding to one of the active irreducible representations satisfying the criteria for a second-order phase transition

Critical irreducible representation	Critical order parameter	Symmetry space group of the distorted phase	Basis vectors*
L_3^+ (9–5)	(η, η, 0, 0, 0, 0, 0, 0)	$C2/m$	(1/2, 1/2, −1) (−1/2, 1/2, 0) (1/2, 1/2, 1)
L_3^+ (9–5)	(η, −η, 0, 0, 0, 0, 0, 0)	$C2/c$	(1/2, 1/2, −1) (−1/2, 1/2, 0) (1/2, 1/2, 1)
L_3^- (9–6)	(η, η, 0, 0, 0, 0, 0, 0)	$C2/m$	(1/2, 1/2, −1) (−1/2, 1/2, 0) (1/2, 1/2, 1)
L_3^- (9–6)	(η, −η, 0, 0, 0, 0, 0, 0)	$C2/c$	(1/2, 1/2, −1) (−1/2, 1/2, 0) (1/2, 1/2, 1)
X_5^- (10–10)	(η, 0, 0, 0, 0, 0)	$Pmmn$	(1/2, 0, 1/2) (0, 1, 0) (−1/2, 0, 1/2)
X_5^- (10–10)	(η, η, 0, 0, 0, 0)	$Cmcm$	(0, 0, 1) (1, 0, 0) (0, 1, 0)

* Basis vectors are given in terms of cubic unit cell parameters.

(1 4 4) superstructure reflection in the angle range of 59.4°. There remain two orthorhombic unit cells (Table 1), which are responsible for the superstructure reflection in this angle range in the X-ray diffraction pattern.

These orthorhombic unit cells differ from each other by the orientation of their own axes with respect to the axes of the cubic unit cell of the G_0 undistorted phase. The orthorhombic unit cell *Pmmn* has two own axes aligned along the diagonals of the faces of the cubic unit cell, whereas all three axes of the orthorhombic unit cell *Cmcm* are directed along the former fourfold axes of the cubic unit cell. Following the homology method [6], it can be shown that the splittings of the principal reflections in the X-ray diffraction patterns of these two unit cells differ from each other. In particular, the (*h h h*) reflection of the cubic unit cell should be split into two reflections in the orthorhombic space group *Pmmn* and should remain nonsplit in the orthorhombic space group *Cmcm*. In this case, the (*h* 0 0) reflection is split into two reflections in the orthorhombic space group *Pmmn* and into three reflections in the orthorhombic space group *Cmcm*. In our case, the (*h h h*) reflections (Fig. 1a) become slightly broadened, while the (*h* 0 0) reflections are described fairly well by only two reflections in the full-profile refinement, which indicates the orthorhombic space group *Pmmn* with a high degree of accuracy.

Thus, among all possible symmetry variants, only the variant of the orthorhombic space group *Pmmn* of the G_1 distorted phase satisfies the requirement of the second-order phase transition, the presence of a superstructure in particular ranges, and the splitting of the principal reflections. Therefore, it can be argued that the symmetry of the distorted phase of the $(NH_4)_2KWO_3F_3$ crystal, which was determined in [4] as $P2_1/n$, is most likely erroneous.

It can be seen from Table 1 that the symmetry change $Fm\bar{3}m \longrightarrow Pmmn$ is associated with the appearance of the phenomenological order parameter, which is transformed according to the irreversible representation X_5^- (10–10) of space group $Fm\bar{3}m$ with the wave vector of the Brillouin zone center (point *X*, $\mathbf{k}_{10} = 1/2(\mathbf{b}_2 + \mathbf{b}_3)$). All notations regarding the irreversible representations and points of the Brillouin zone are given in accordance with the reference book [9]. Following [10], these order parameters, which specify the symmetry of the distorted phase, as well as the order-related structural distortions, atomic displacements, and atomic orderings, will be referred to as critical.

The structural model of the G_1 distorted phase was determined using the traditional Patterson function method and the symmetry analysis of the structure of the G_0 parent phase [11]. The symmetry analysis includes an analysis of the mechanical and permutation representations and allows one to assume possible displacements and orderings of ions in the distorted phase when the critical order parameter and the critical irreversible representation are known. The critical displacements and the probabilities that atoms can occupy one or other position in the unit cell are determined during the refinement of the crystal structure. This possibility is implemented in the BRUKER-AXS TOPAS 4 program [11].

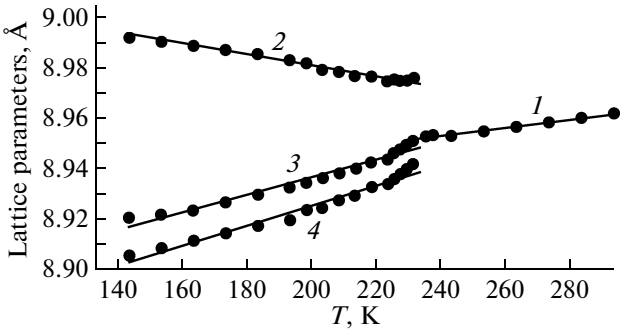

Fig. 4. Temperature dependences of the unit cell parameters of (*1*) the G_0 cubic phase a_0 and (*2–4*) the G_1 orthorhombic phase (*2*) b_1, (*3*) $a_1\sqrt{2}$, and (*4*) $c_1\sqrt{2}$ of the $(NH_4)_2KWO_3F_3$ compound.

As was noted above, the atomic coordinates, the occupancies of their positions, and the thermal parameters were refined using the data obtained from the experiments performed at temperatures of 298 and 133 K, i.e., in the cubic and orthorhombic phases. The refinement was carried out according to a new procedure that has not yet widely used now and implemented in the DDM program [12]. In parallel, the temperature dependences of the parameters of the reduced cubic unit cell (Fig. 4) were determined during fitting of the profiles of the X-ray diffraction patterns obtained at other temperatures. The shapes of the peaks were described by the Pearson VII function.

In the high-temperature cubic phase G_0 at a temperature of 298 K, the $(NH_4)_2KWO_3F_3$ crystal has the elpasolite structure [4]. The refinement of the structure according to the data obtained in [4] led to the satisfactory *R* factors; however, the thermal parameter of the nitrogen atom had a very low value of ~0.07 Å^2. Earlier [4], it was mentioned that the refinement of the thermal parameter of this atom is unstable. In [4], the thermal parameter of the nitrogen atom during the refinement was fixed. In the present work, where the exposure was increased by several orders of magnitude, the effect should seemingly be lost. However, it persisted. Therefore, it was assumed that there is an insignificant nonstoichiometry of the composition of the crystal. It is most probable that the position occupied by the nitrogen atom also contains a small amount of potassium. The occupancy of the position

Table 2. Data collection and structure refinement parameters of the $(NH_4)_2KWO_3F_3$ compound

Parameter	$T = 298$ K	$T = 133$ K
Space group	$Fm\bar{3}m$	$Pmmn$
a_i, Å	a_0, 8.96124(9)	$1/2(a_0 + c_0)$, 6.3036(3)
b_i, Å	b_0, 0.96124(9)	b_0, 8.9891(3)
c_i, Å	c_0, 8.96124(9)	$1/2(-a_0 + c_0)$, 6.2976(4)
V, Å^3	719.62(1)	356.85(3)
Z	4	1
2θ angle range, deg	5–110	5–110
Number of reflections	39	271
Number of parameters refined	8	22
R_B, %	3.36	5.79
R_{DDM}, %	12.07	14.84
Order parameter η	(0, 0, 0, 0, 0, 0)	(η, 0, 0, 0, 0, 0)

Note: R_B is the Bragg integral discrepancy factor, and R_{DDM} is the profile discrepancy factor determined with the DDM program [12].

with these atoms was refined so that its total value would remain equal to unity. After these transformations, the thermal parameters of the nitrogen and potassium atoms took on a normal value. As a result, the position of the nitrogen atom contained approximately 8% of the potassium atoms. Consequently, the true composition of the compound should be written as $[(NH_4)_{0.925(7)}K_{0.075(7)}]_2KWO_3F_3$. The final results of the structure refinement of the G_0 cubic phase are presented in Tables 2 and 3. The selected bond lengths are listed in Table 4.

In the refinement of the structure of the G_1 phase at a temperature of 133 K, by analogy with the cubic phase, the potassium atom was also placed in the position occupied by the nitrogen atom. The refinement of the structure led to an almost twofold increase in the percentage of the potassium atoms in this position (~14%); however, the obtained difference in the concentrations falls within four standard deviations. The coordinates of the hydrogen atoms and the ammonium ion were determined theoretically with the ISODISPLACE software package [8] and refined together with all the other atomic coordinates. The thermal parameters of the hydrogen atoms and F2(O2) were fixed to decrease the number of the parameters refined. The refinement of this model was stable and led to low values of the discrepancy factor R (Tables 2, 3). The selected bond lengths are presented in Table 4.

4. DISCUSSION OF THE RESULTS

For the understanding of the mechanism of the phase transitions and the separation of leading (critical) atoms, we will simulate the ordering of the WO_3F_3 octahedron, which, according to the data reported in [13, 14], has the symmetry $3mm(C_{3v})$. For this purpose, we will act as was done in our recent work [15]. Since the d(W–O) and d(W–F) distances differ from each other, the WO_3F_3 octahedron can be represented as a vector directed from the center of the triangle built on the F atoms to the center of the triangle built on the O atoms. In the cubic unit cell, the WO_3F_3 octahedron is oriented so that this vector has the coordinates (x, x, x); i.e., it is in the position 32f of the face-centered cubic unit cell. By replacing the octahedron with the vector, it is easy to obtain the number of different orientations of WO_3F_3 in the cubic phase. Since the (x, x, x) position in the cubic phase has a multiplicity of 32, the number of orientations of WO_3F_3 in a particular site is $N_0 = 32/Z = 32/4 = 8$, where $Z = 4$ is the number of formula units in the face-centered cubic unit cell. Thus, in the cubic phase, there are eight different orientations of the WO_3F_3 octahedron or the vector replacing the WO_3F_3 octahedron.

By using the group-theoretical analysis of the permutation representation, it is easy to determine how the occupancies of these eight positions change with the symmetry transformation $Fm\bar{3}m \longrightarrow Pmmn$ and, consequently, to elucidate which of the orientations of the octahedron are energetically more favorable after the phase transition when the critical order parameter is known.

For these purposes, it is most convenient to use the ISODISPLACE software package [8], because it visualizes the obtained result. As was already noted above, the change in the symmetry during the phase transition in the $(NH_4)_2KWO_3F_3$ crystal is caused by the critical six-component order parameter, which is transformed according to the representation X_5^- (10–10). During the phase transition $Fm\bar{3}m \longrightarrow Pmmn$, only one of the six components of the order parameter has a nonzero value: (η, 0, 0, 0, 0, 0) (Table 2). An

Table 3. Atomic coordinates, isotropic thermal parameters (B_{iso}), and position occupancies (p) in the $(NH_4)_2KWO_3F_3$ structure

Atom	p	X	Y	Z	B_{iso}, Å^2
			$T = 298$ K, $Fm\bar{3}m$		
W	1.0	0	0	0	1.82(4)
K	1.0	1/2	1/2	1/2	1.3(1)
N	0.925(7)	1/4	1/4	1/4	2.8(1)
H	0.925(7)	0.192	0.192	0.192	4
K'	0.075(7)	1/4	1/4	1/4	2.8(1)
F	0.5	0.2098(7)	0	0	$U_{11} = U_{22} = 0.025(1)$ $U_{33} = 0.005$ $B_{iso\ equiv} = 5.78$
O	0.5	0.2098(7)	0	0	$U_{11} = U_{22} = 0.025(1)$ $U_{33} = 0.005$ $B_{iso\ equiv} = 5.78$
			$T = 133$ K, $Pmmn$		
W	1.0	3/4	3/4	0.7520(6)	1.16(4)
K	1.0	3/4	1/4	0.743(2)	0.4(1)
N	0.86(2)	1/4	−0.006(9)	0.758(4)	2.5(6)
H1	0.86(2)	0.146	0.939(9)	0.760(4)	4.0
H2	0.86(2)	1/4	0.043(9)	0.639(4)	4.0
H3	0.86(2)	1/4	0.043(9)	0.864(4)	4.0
K'	0.14(2)	1/4	−0.006(9)	0.758(4)	2.5(6)
F1	1.0	−0.046(6)	3/4	0.514(4)	7.7(9)
O1	1.0	0.501(5)	1/4	0.103(4)	1.4(6)
O2	0.5	3/4	−0.044(2)	0.823(6)	1.5
F2	0.5	3/4	−0.044(2)	0.823(6)	1.5

analysis of the structure of the orthorhombic phase G_1 has demonstrated that several O and F atoms are ordered during the phase transition. It is these enumerated orderings and displacements of the atoms that are critical and they are transformed according to the representation X_5^- (10–10) with the order parameter (η, 0, 0, 0, 0, 0). Hence, it is easy to determine which of the orientations of the WO_3F_3 octahedron are realized with a higher probability after this phase transition. Such a model of the ordering of WO_3F_3 polyhedra is presented in Fig. 5. It can be seen from this figure that, after the phase transition, there exist several states with different probabilities. For similar cases, there is a theory of order–disorder phase transitions in which structural elements move in multiple-well potentials [16–18]. In our case, this theory can be used to calculate, for example, the changes in the entropy of the phase transition.

In a number of cases, the distortion of the structure of the parent phase cannot be described only by the critical order parameters. In the distorted (disymmetric) phase, there can occur atomic displacements or

Table 4. Characteristic bond lengths in the $(NH_4)_2KWO_3F_3$ structure

$T = 298$ K		$T = 133$ K	
bond	length, Å	bond	length, Å
W–F(O)	1.880(6)	W–F1	1.97(3)
		W–O1	1.83(3)
		W–F2(O2)	1.90(2)
K–F(O)	2.601(6)	K–F1	2.47(3)
		K–O1	2.76(2)
		K–F2(O2)	2.69(2)
N(K')–F(O)	3.189(4)	N(K')–F1	3.14(3)
		N(K')–O1	2.84(3)
		N(K')–F2(O2)	3.196(7)
N–H	0.90	N–H1	0.82(2)
		N–H2	0.87(4)
		N–H3	0.80(4)

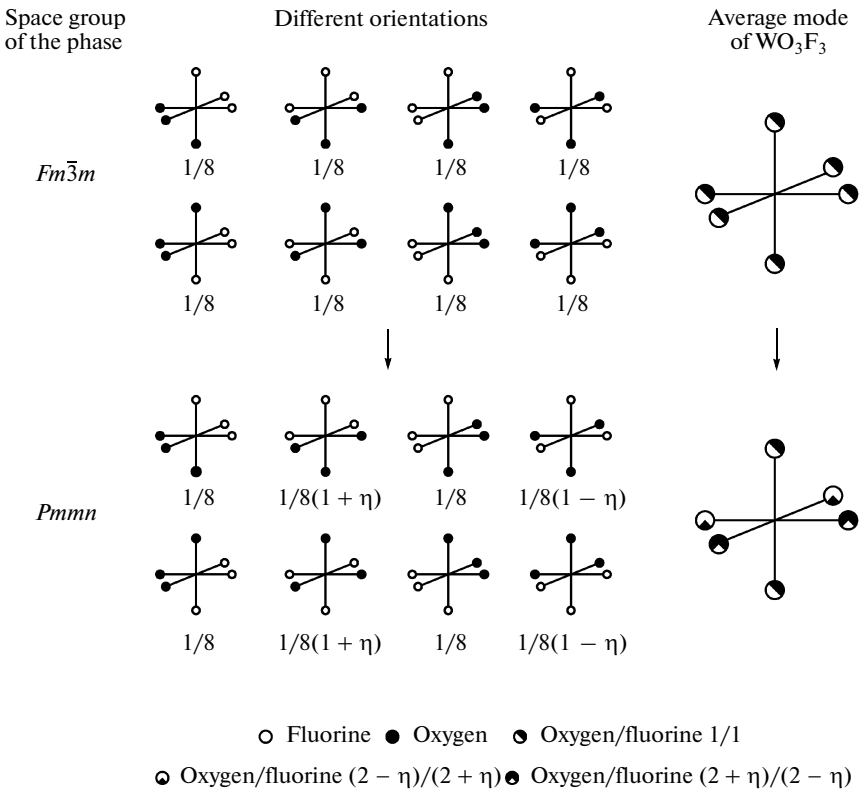

Fig. 5. Model of the ordering of the WO_3F_3 polyhedra in the C_{3v} configuration. Numbers under the particular orientation of the polyhedron indicate the probability of its existence; η is the critical order parameter, which is transformed according to the X_5^- representation.

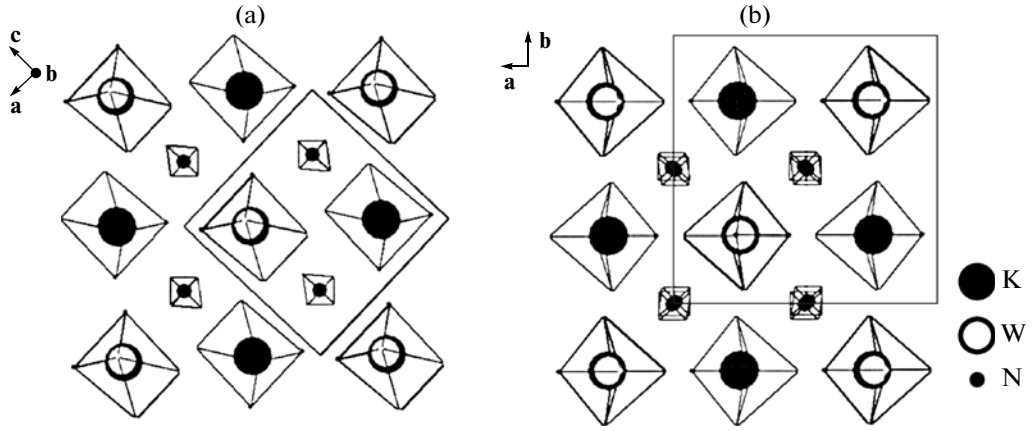

Fig. 6. Projections of the structure of the G_1 distorted phase of the $(NH_4)_2KWO_3F_3$ compound (a) along the former cubic axis $\mathbf{b}_0$ and (b) along the former cubic axis $\mathbf{c}_0$.

orderings that are compatible with the symmetry of this phase and which are specified by the noncritical (secondary) order parameters and irreducible representations. The entire set of order parameters, both critical and noncritical, which appear during the phase transition, forms the complete order parameter condensate [10]. The noncritical distortions have a secondary character and are insignificant in the vicinity of the phase transition points. The symmetry analysis indicates only the presence and type of noncritical order parameters. The numerical values of both the critical and noncritical distortions and order parame-

ters involved in the complete condensate are determined from the experimental and, primarily, structural data.

The critical irreducible representation (10–10)(X_5^-) is related to the noncritical irreducible representations 11–3(Γ_2^+), 11–5(Γ_3^+), 11–7(Γ_5^+), 10–1(X_1^+), 10–7(X_4^+), and 10–9(X_5^+). The noncritical irreducible representation 11–7(Γ_5^+) most actively manifests itself. For example, the ordering is accompanied by a small displacement of the K, W, and N atoms with respect to their positions in the cubic unit cell: Δr(W) = (–0.009, 0, 0.009) Å, Δr(K) = (0.031, 0, –0.031) Å, and Δr(N) = (0.036, –0.054, 0.036) Å (hereinafter, the components of all atomic displacements are given with respect to the pseudocubic cell) (Fig. 6). in this case, the displacement of the nitrogen atom by Δr(N) = (0, –0.054, 0) Å is caused by precisely the noncritical irreducible representation 11–7(Γ_5^+). The other displacements Δr(W) = (–0.009, 0, 0.009) Å, Δr(K) = (0.031, 0, –0.031) Å, and Δr(N) = (0.036, 0, 0.036) Å are the critical displacements caused by the critical irreducible representation (10–10)X_5^-. The displacements of the F and O atoms are more complex but also predominantly occur under the action of the critical (10–10)X_5^- and noncritical 11–7(Γ_5^+) irreducible representations; in this case, unlike the nitrogen atom, the amplitudes of the noncritical displacements are smaller than those of the critical displacements.

5. CONCLUSIONS

Thus, the structural transformation in the $(NH_4)_2KWO_3F_3$ crystal, which can be schematically represented as $Fm\bar{3}m \xrightarrow[(\eta, 0, 0, 0, 0, 0)]{10-10(X_5^-)} Pmmn$, has been revealed using X-ray powder diffraction in combination with the appropriate procedures of symmetry analysis of the complete order parameter condensate. The leading critical transformation in the structure is the ordering of the WO_3F_3 polyhedron related to the critical order parameter (η, 0, 0, 0, 0, 0) of the representation 10–10(X_5^-). The most pronounced noncritical distortion is the displacement of the ammonium ion, which is transformed according to the noncritical representation 11–7(Γ_5^+).

ACKNOWLEDGMENTS

We would like to thank Professor V.I. Zinenko for helpful discussions of the results obtained in this work.

This study was supported by the Council on Grants from the President of the Russian Federation for Support of Leading Scientific Schools of the Russian Federation (grant no. NSh-4645.2010.2).

REFERENCES

1. I. N. Flerov, M. V. Gorev, K. S. Aleksandrov, A. Tressaud, J. Grannec, and M. Couzi, Mater. Sci. Eng., R **24**, 81 (1998).
2. J. Ravez, G. Peraudeau, H. Arend, S. C. Abrahams, and P. Hagenmuller, Ferroelectrics **26**, 767 (1980).
3. I. N. Flerov, M. V. Gorev, V. D. Fokina, A. F. Bovina, M. S. Molokeev, Yu. V. Boiko, V. N. Voronov, and A. G. Kocharova, Phys. Solid State **48** (1), 106 (2006).
4. M. S. Molokeev, A. D. Vasiliev, and A. G. Kocharova, Powder Diffr. **22**, 227 (2007).
5. K. S. Aleksandrov, S. V. Misyul, and E. E. Baturinets, Ferroelectrics **354**, 60 (2007).
6. V. I. Mikheev, *X-Ray Determination of Minerals* (Geologiya i Okhrana Nedr, Moscow, 1957) [in Russian].
7. H. T. Stokes, D. M. Hatch, and B. J. Campbell, *ISOTROPY: Program for Displaying Information about Space Groups, Irreducible Representations, Isotropy Subgroups, and Phase Transitions* (Department of Physics and Astronomy Brigham Young University, Provo, Utah, United States, 2007); stokes.byu.edu/isotropy.html.
8. B. J. Campbell, H. T. Stokes, D. E. Tanner, and D. M. Hatch, J. Appl. Crystallogr. **39**, 607 (2006).
9. O. V. Kovalev, *Irreducible and Induced Representations and Co-Representations of Fedorov's Groups* (Nauka, Moscow, 1986) [in Russian].
10. V. P. Sakhanenko, V. M. Talanov, and G. M. Chechin, Fiz. Met. Metalloved. **62**, 847 (1986).
11. R. W. Cheary, A. A. Coelho, and J. P. Cline, J. Res. Natl. Inst. Stand. Technol. **109**, 1 (2004).
12. L. A. Solovyov, J. Appl. Crystallogr. **37**, 743 (2004).
13. E. I. Voit, A. V. Voit, A. A. Mashkovskii, N. M. Laptash, and V. Ya. Kavun, J. Struct. Chem. **47** (4), 642 (2006).
14. A. S. Krylov, Yu. V. Gerasimova, A. N. Vtyurin, V. D. Fokina, N. M. Laptash, and E. I. Voit, Phys. Solid State **48** (7), 1356 (2006).
15. M. S. Molokeev, S. V. Misyul', V. D. Fokina, A. G. Kocharova, and K. S. Aleksandrov, Phys. Solid State **53** (4), 834 (2011).
16. D. Ya. Badalyan, Sov. Phys. Crystallogr. **14** (1), 36 (1969).
17. D. Ya. Badalyan, Sov. Phys. Crystallogr. **14** (3), 333 (1969).
18. A. G. Khachaturyan, *Theory of Phase Transitions and the Structure of Solid Solutions* (Nauka, Moscow, 1974) [in Russian].

Translated by O. Borovik-Romanova